

SUMMER PRECIPITATION ONTO THE SOUTH POLAR PLATEAU

Masayuki INOUE¹, Takeshi OHTAKE² and Gorow WAKAHAMA³

¹*Applied Meteorological Engineering and Consulting Services, Co.,
Sato Bldg., 1-8, Ueno 3-chome, Taito-ku, Tokyo 110*

²*Geophysical Institute, University of Alaska, Fairbanks, Alaska 99701, U.S.A.*

³*The Institute of Low Temperature Science, Hokkaido University,
Kita-19, Nishi-8, Kita-ku, Sapporo 060*

Abstract: A study was made of ice crystal precipitation in austral summer 1978–1979 at the South Pole from analyses of data of meteorological observations, in which low-level micrometeorological elements were measured by conventional apparatus and high-altitude elements were measured by radiosondes. The result shows that ice crystal precipitation can be classified into “clear sky precipitation” and precipitation from clouds. The latter plays a dominant role in net accumulation of snow at and near the South Pole. In this case moist air masses move inland in advective flow along the surface of Antarctica from the Weddell and Ross Seas and cool down to form stratus-type clouds from which ice crystals fall at the South Pole. The former, on the other hand, presents an interesting phenomenon, as ice crystal precipitation falls from a clear sky. This study has disclosed that it originates in a layer which is supersaturated with respect to ice, located slightly above the ground surface, and too thin to be identified as a stratus cloud. It will be sufficient to consider that the former represents a short-life transition from the absence of precipitation from a clear sky to precipitation from clouds and *v.v.*; hence, it cannot play an important role in net accumulation of snow there.

1. Introduction

Atmospheric ice crystals at South Pole Station have been studied since December 1974 to clarify their mechanisms of precipitation and their influence on the Antarctic climate. Because ice crystal precipitation is the only way to remove water vapor from the Antarctic atmosphere toward the inland ice sheet, some knowledge of formation mechanisms and rate of precipitation is necessary to understand the budget of atmospheric water vapor.

Atmospheric ice crystals, which are frequently observed in the polar regions, were observed on 317 days out of 360 days in central Antarctica (KUHN, 1970). But the amount of water vapor is very likely limited, because the source mostly originates in and is transported from the surrounding seas.

It is known that net accumulation of snow totals annually an equivalent about of 5 to 10g of water per unit area at the South Pole, but the mechanism of precipitation onto the South Polar Plateau is still open to question. HOGAN (1979) indicated that the highest concentration of aerosol particles over the South Polar Plateau was found in the lower layers immediately above the surface inversion layer and they were transported there from the seas. Meanwhile, SCHWERDTFEGGER (1969), who estimated

the amount of moisture which produces ice crystals at the South Pole, suggested that an explanation was given by warm air in advective flow from lower latitudes thereto as an adequate source of ice crystals which were formed as the air cooled down. Moreover, LAX and SCHWERDTFEGER (1976) reported that the occurrence of ice crystals at the South Pole was associated with winds from 225° to 45° in azimuth, which caused warm air flow to rise along the slope.

The occurrence of ice crystal precipitation near the snow surface under the apparently cloudless sky is not rare in cold regions. This precipitation has been reported by ITOO (1951) in Manchuria, by OHTAKE and JAYAWEERA (1972) in Fairbanks, Alaska, and by OHTAKE and HOLGREN (1974) in an Arctic coastal area. According to RUSIN (1964), ice crystal precipitation from a clear sky may account for 20 to 30 percent of the annual accumulation of snow at Vostok Station, East Antarctica. But their mechanism of formation is not always clear.

It is then indispensable to look into what multiple effects ice crystal precipitation has on the mass and heat balance. In this connection, RUBIN and WEYANT (1963) studied the mass budget of the Antarctic atmosphere, which represents a consistent pattern of outflow in the lower troposphere and inflow in both the upper troposphere and lower stratosphere. This conceptually simple model is in agreement with a postulation from an ozone transport value (WEXLER *et al.*, 1960) and with the result of an analysis of daily upper-air data over different sectors of the continent (KUTZBACH and SCHWERDTFEGER, 1967).

The authors' current research into Antarctic ice crystals, which has been continued over four years, is near completion. The data of atmospheric ice crystals at South Pole Station were obtained by OHTAKE and INOUE (1980) and were used to work out a hypothesis describing meteorological mechanisms responsible for transport of water vapor to the South Polar Plateau. The results are summarized as an introduction to this work. That is, ice crystals are formed in the following three different layers in the austral summer:

- 1) High-level clouds (cirrus; cirrostratus): large assembled-bullet ice crystals (one mm or larger in size).
- 2) Middle-level clouds (altostratus; altocumulus): combined ice crystals in the forms of side plates, bullets and columns (about one mm in size).
- 3) The lowest-level atmosphere between the snow surface and the altitude of 500 m, which has no visible cloud layer though accompanied by fractostratus sometimes; ice crystals in the forms of thin hexagonal plates and columns (smaller than 0.2 mm in size).

A series of investigations reported here was carried out from November 1978 to January 1979 by measuring low-level micrometeorological elements above the South Pole as well as making high-altitude observations by radiosondes, in an attempt to find mechanisms of ice crystal precipitation at the South Pole and its vicinity.

2. Humidity Measurement

It has been pointed out that at South Pole Station the radiosonde gave lower values of surface humidity than the dew-point hygrometer *in situ*. The authors found

out that the difference derived from not having adjusted the radiosonde to the altitude of the South Pole, 2854 m above mean sea level. Hence, before the ascension of a balloon a correction was made in the radiosonde humidity element calibration so that this altitude was taken into account. As a result, the radiosonde showed almost the same value as the hygrometer.

To confirm the radiosonde data above South Pole Station, the authors performed seeding experiments using dry ice pellets suspended from the radiosonde balloon in the same way as KIKUCHI and HOGAN (1976); the experiment made it possible to detect vapor supersaturated with respect to ice, where dense ice contrails issued forth. Calibration of the humidity element was made possible by a comparison between the height of supersaturated layers obtained from radiosonde observations and the height obtained from seeding experiments.

The result of a radiosonde observation conducted on December 28, 1978 is, as an example, transferred to a Skew-T, Log-P diagram in Fig. 1, together with the result of a seeding experiment done at the same time that is shown in the column of the figure noted as DRY ICE. In the figure, solid circles correspond to temperatures (T); open triangles and open circles correspond, respectively, to apparent mixing ratios (T_i) calculated from atmospheric pressures and temperatures and real mixing ratios (T_d) obtained by correcting the observed humidity altimetically.

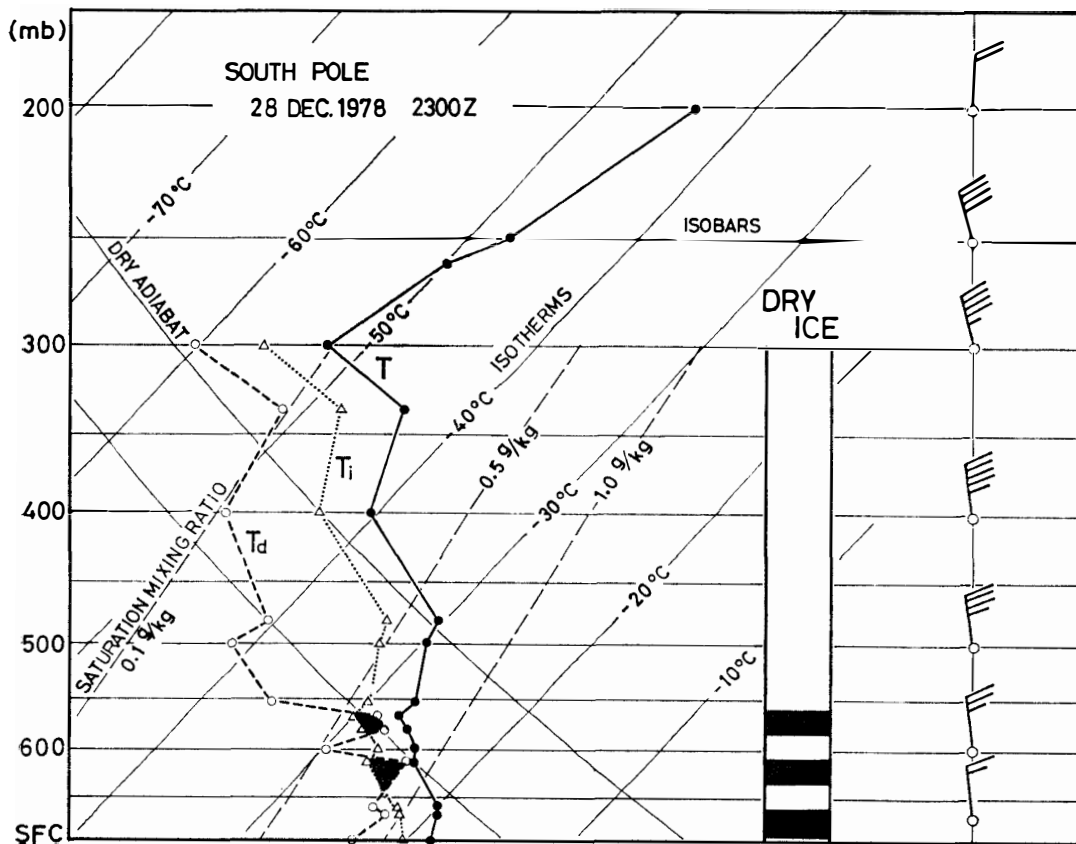


Fig. 1. The result of a radiosonde observation conducted on December 28, 1978 plotted on a Skew-T, Log-P diagram. Each full bar of the wind symbol represents 5 m/s.

In the column noted as DRY ICE there are three shaded layers, where the dense contrails were observed. Upon correction for humidity sensor hysteresis, close agreement was found between heights of the contrail layer measured from the seeding experiment and the supersaturated layer calculated from atmospheric pressures, temperatures and humidities above the South Pole. A discrepancy at the bottom layers does not contradict the previous statement, because it is attributable to the handling error resulting from a failure in adapting the humidity sensor thoroughly to the atmosphere before radiosonde ascent. Therefore, the authors concluded that the humidity data obtained from the radiosonde observations at the South Pole are fit for analysis.

In attacking the problem of ice crystal precipitation it is natural to introduce the idea of precipitable water in a vertical column of air. The volume dW_p of liquid water equivalent to an air column of depth dZ and a unit cross-sectional area is $dW_p = r \cdot \rho \cdot dZ$, where r is the mixing ratio and ρ is the density of air. Upon substitution from the hydrostatic equation and then integrations,

$$\int_{P_1}^{P_2} dW_p = (1/g) \int_{P_1}^{P_2} r \cdot (-dP),$$

where g is the acceleration of gravity. Thus, the depth of precipitable water W_p (mm) in a layer of given pressures between P_1 and P_2 is obtained by evaluating the average mixing ratio in the layer.

Ice crystals grow within a moist layer supersaturated with respect to ice. Such a layer is nearly equivalent to a cloud layer. Then, suppose that the amount of water vapor in it is larger than the amount of water vapor saturated with respect to ice under the present air pressure and temperature. Subtract the latter from the former, and we have a residue. The residue serves as a measure of the existence of a cloud, which will be transformed into ice crystal precipitation. For making the meaning distinct, the authors will use the term "precipitable ice" instead of precipitable water.

3. Results

3.1. Surface meteorological observations at the South Pole

Very little is known of ice crystal precipitation and cloud distribution in both coastal zones and interior regions of Antarctica, because no means has been devised to record precipitation there, precipitation onto the continent falling almost entirely as ice crystals or snow. An ordinary snow gauge is effective only when the ambient air is calm; when it is not, the gauge is not effective, because drifting and falling snow particles enter the gauge. Alteration of flow due to the presence of the gauge itself also affects the measurements. Difficulty in determining whether or not snow is actually falling increases the uncertainty of the results. Although this problem was too difficult to solve perfectly, a fair approach was adopted to detect ice crystal precipitation at the South Pole as follows:

The concentration of ice crystals was continuously recorded at a rooftop about 10 m above the snow surface from December 7, 1978 to January 10, 1979 using an acoustic ice crystal sensor (OHTAKE, 1976), which is so structured that ice crystals

smaller than 20 microns in size, which represents the size of fog droplets and air pollution particles, do not trigger the sensor. Moreover, an ice crystal replicator, originally designed by HINDMAN and RINKER (1967), was employed to record the shape, size and concentration of ice crystals. The concentration varied widely by as much as four orders of magnitude during the observation period. The maximum was roughly ten crystals per liter of air on December 26, 1978.

The meteorological conditions at the South Pole are shown in Fig. 2 by time sections of various surface elements measured at intervals of twelve hours from November 1, 1978 to January 23, 1979. Air pressure, air temperature, and both the easterly (U) and northerly (V) wind components were obtained by C.S.I.R.O.; relative humidity (R.H.) was obtained by the authors using a dew-point hygrometer about 5 m above the snow surface.

Judging from measurements both with the acoustic sensor and by eye, whether or not clear sky precipitation occurred was determined. When occurrence was confirmed at a routine observation time, it was indicated by a vertical broken line in the bottom frame of the figure.

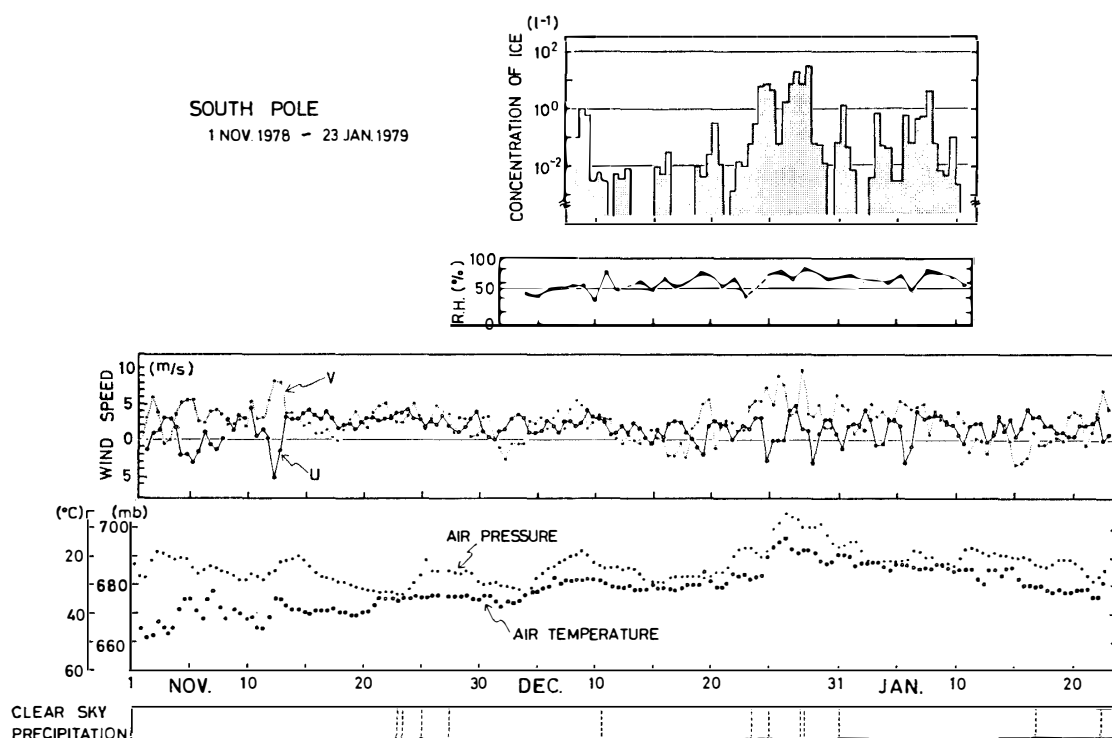


Fig. 2. Meteorological surface elements at the South Pole from November 1, 1978 to January 23, 1979 are shown by time sections.

3.2. Clear sky precipitation at the South Pole

For a study of "clear sky precipitation" it is necessary to elucidate the structure of water vapor in the low troposphere. In effect, a conventional radiosonde rising at a speed of 4 to 6 m/s was found not fit for a detailed study of the structure of water vapor near the snow surface. Then, the authors conducted eleven detailed

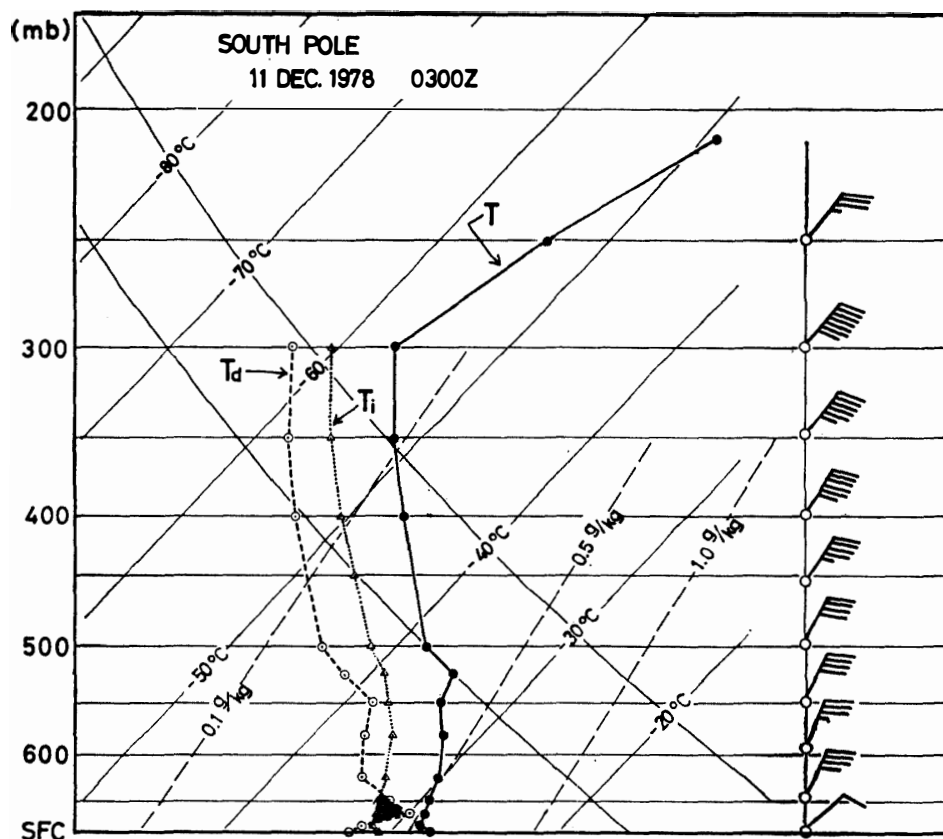


Fig. 3. A Skew-T, Log-P diagram shows the shaded area of clear sky precipitation detected by a detailed radiosonde observation at 0300 GMT, December 11.

observations using radiosondes, filling the balloon with helium gas to only half its volume. Of the eleven trials, only one was able to detect clear sky precipitation. This rarity results from the short lifetime of ice crystal formation, say, several hours.

Plate-type ice crystals were precipitated from a cloudless sky, which had an ice crystal concentration of about 10^{-3} per liter of air at 0300 GMT, December 11, 1978. This clear sky precipitation was detected successfully by a detailed radiosonde observation, as shown in Fig. 3. A layer shaded from 740 to 675 mb in the Skew-T, Log-P diagram supersaturated with respect to ice. The layer had a thickness of roughly 400 m. The amount of precipitable ice contained within the layer was equivalent to 0.014 mm of water per unit area. It is, therefore, natural to consider that the existence of a layer supersaturated with respect to ice near the snow-covered surface constitutes a necessary condition for clear sky precipitation.

Figure 4 shows the humidity fields, expressed as a linear relation of height vs. mixing ratio, before, during, and after clear sky precipitation, which was calculated from routine radiosonde observations. As for the weather, the sky cleared up with no precipitation falling from a cloudless sky at 0200 GMT, December 10. Then ice crystals began to fall from a cloudless sky at 0200 GMT, and stopped at 0600 GMT on the 11th. Ice crystals were precipitated from altostratus and cirrostratus after 1100 GMT on the 11th. During the precipitation, halos were noticed. The cloud amount was two-tenths at 1100 GMT, the routine observation time. The altitudes

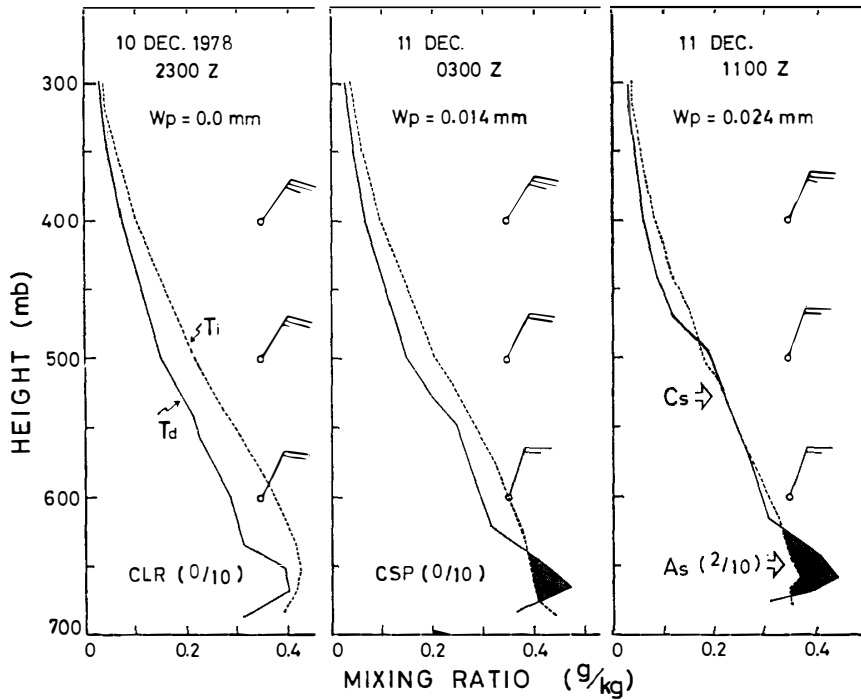


Fig. 4. Humidity fields, expressed as a linear relation of height vs. mixing ratio, before, during, and after clear sky precipitation.

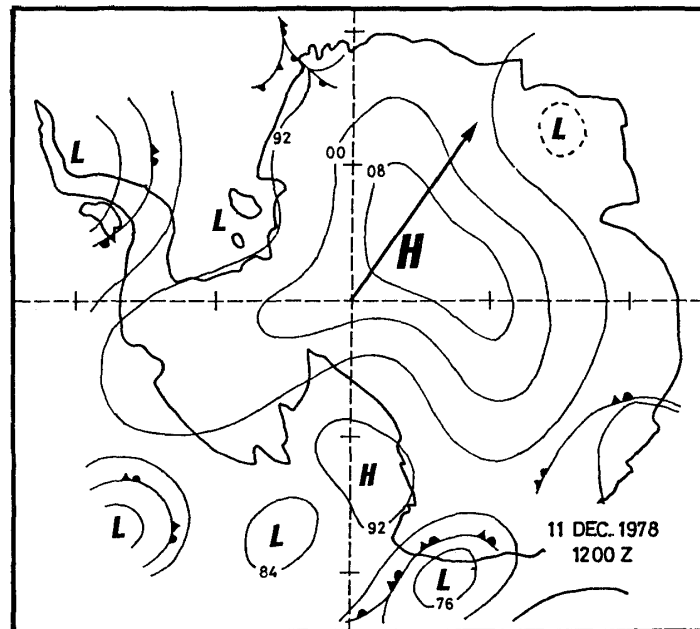


Fig. 5. A sea-level pressure chart at 1200 GMT, December 11, with a thermal wind direction within the level from 600 to 300 mb shown by an arrow.

of cloud bottoms, which were observed routinely with the naked eye, are shown by arrows in the figure.

As can be foreseen, a sequence of precipitation can be elucidate by the existence of layers supersaturated with respect to ice; no precipitation from a cloudless sky; precipitation from a cloudless sky; precipitation from clouds. They imply, respectively, the absence of a layer supersaturated with respect to ice; a thin layer supersaturated with precipitable ice equivalent to 0.014 mm of water per unit area; a thick layer supersaturated with precipitable ice equivalent to 0.024 mm.

A sea-level pressure chart at 1200 GMT on the 11th is shown in Fig. 5. It is seen that a polar anticyclone, characteristic of Antarctic meteorology, was dominant over the interior core region.

Figure 6 shows a hodograph of geostrophic winds in the troposphere when clear sky precipitation occurred at 0300 GMT on the 11th. A hodogram segment between 600 and 300 mb shows a special feature of a straight thermal wind vector. That is, the thermal wind direction and thermal wind speed $(C_n)_g$ within the layer bounded by the two isobaric surfaces can be computed to be constantly 50° in azimuth and 4.9 m/s, respectively. Isotherms which veered into an easterly direction from 600 to 300 mb indicate that a cold air mass moved in advective flow from the interior

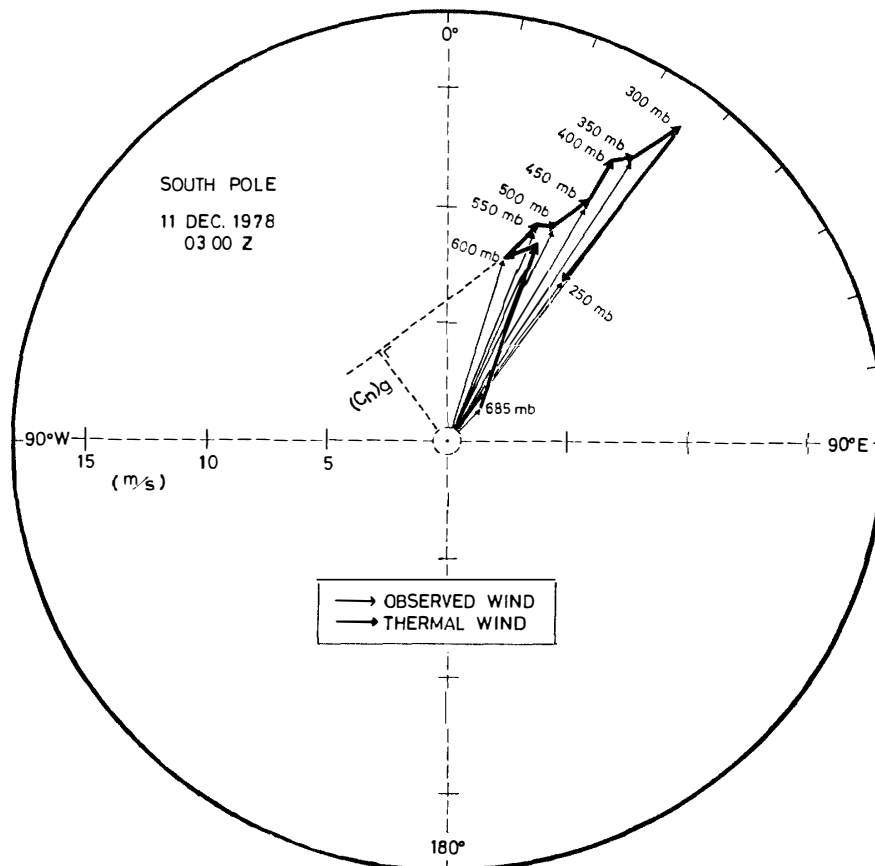


Fig. 6. A hodograph of geostrophic winds in the troposphere with clear sky precipitation at 0300 GMT, December 11.

region to the South Polar Plateau. The authors consider that a little water vapor was contained in the air mass, which was transported over a long distance across the highest interior region from the Indian Ocean.

When ice crystal precipitation occurred from a cloudless sky and from a cloudy sky, both the geographic winds and the thermal winds became gradually weak and eastward. In case of precipitation from clouds at 1100 GMT on the 11th there were lighter westward winds and smaller vertical wind shears between the 650–500 mb lever and veering winds aloft, northwest of the main northeasterly current below and the cold advection current above. Meanwhile, during the precipitation from clouds at 2300 GMT on the 11th, the winds backed up more westward indicating a warm advection air current. Therefore, the wind variation aloft may be a cause of the difference in precipitation from a cloudless sky and from clouds, cold and warm advection prevailing respectively.

Four routine and one detailed radiosonde observations which detect clear sky precipitation have been selected, and the results tabulated in Table 1. A thin layer is supersaturated with respect to ice near the snow surface in every precipitation case. If a larger amount of water vapor in a supersaturated state with respect to ice is contained in such a thin layer, the layer can be identified by the eye as clouds. It is, therefore, concluded that ice crystals fall from a thin layer supersaturated with respect to ice or a pseudostratus cloud, which appears cloudless to the eye.

Films taken by an all-sky slow-motion movie camera indicate that immediately above the horizon around the South Pole there was always a small amount of stratus, say, less than one tenth, when clear sky precipitation was detected. This phenomenon may be associated with the thickness of the layer supersaturated with respect to ice. At locations without stratus clouds the layer may be too thin in thickness to be visible. If the layer with a constant depth covers a wide area above South Pole Station, its thickness varies in appearance with respect to the angle of the line of vision; namely, the layer looks thicker horizontally than vertically. In other words, the layer looks like stratus if the line of vision is horizontal, but less so, as it deviates from the horizontal.

Table 1. Various items to be taken into account for clear sky precipitation at the South Pole.

	Surface pressure (mb)	Ice saturated layer			W_p (mm)	Inversion layer (mb)	500 mb		Legend
		Lower (mb)	Upper (mb)	Thickness (m)			dd	vv (m/s)	
Nov. 26, 1978 1100 Z	683.3	645 673	600 660	500 140	0.005 0.003	635–683	25°W	15	Routine RAOB
Dec. 11, 1978 0300 Z	685.8	675	638	404	0.014	520–550	26°E	10	Detailed RAOB
Dec. 24, 1978 1100 Z	691.3	653	632	234	0.005	612–638 658–690	10°W	12	Routine RAOB
Jan. 17, 1979 1100 Z	687.1	644 665	637 655	79 172	0.0004 0.0004	630–656	94°E	3	Routine RAOB
Jan. 22, 1979 1100 Z	681.1	680	647	355	0.008	604–620 650–681	27°E	3	Routine RAOB

3.3. Regular precipitation from clouds at the South Pole

Some difference is considered to exist between the formation mechanism of clear sky precipitation and that of regular precipitation from clouds.

Snow showers from stratus clouds were observed after precipitation from a cloudless sky at 0000 GMT, December 24, 1978. Temperatures, mixing ratios and winds aloft are shown in Fig. 7 in precipitation cases from altostratus covering three-tenths of the sky at 2300 GMT on the 24th and from overcast altostratus at 1100 GMT on the 25th. Both cases lasted until the 27th, with drifting snow driven by strong 6 to 8 m/s winds one m above the snow surface.

As shown in the figure, both temperature and humidity increased greatly every twelve hours. The same tendency was observed in the case of precipitable ice within shaded layers varying in depth from 0.007 mm at 2300 GMT on the 24th to 0.087 mm at 1100 GMT on the 25th. The shaded layer came to be saturated with respect to water near the 650-mb level immediately below the temperature inversion layer at 1100 GMT on the 25th, which was remarkable in austral summer at the South Pole.

There were two polar anticyclones over Antarctica, which formed a trough in the NW direction on the surface chart at 1200 GMT on the 25th, as shown in Fig. 8a.

A thermal wind with the constant wind speed of 1.5 m/s at a level from 600 to 350 mb is derived from a hodograph of observed geostrophic winds and shown in

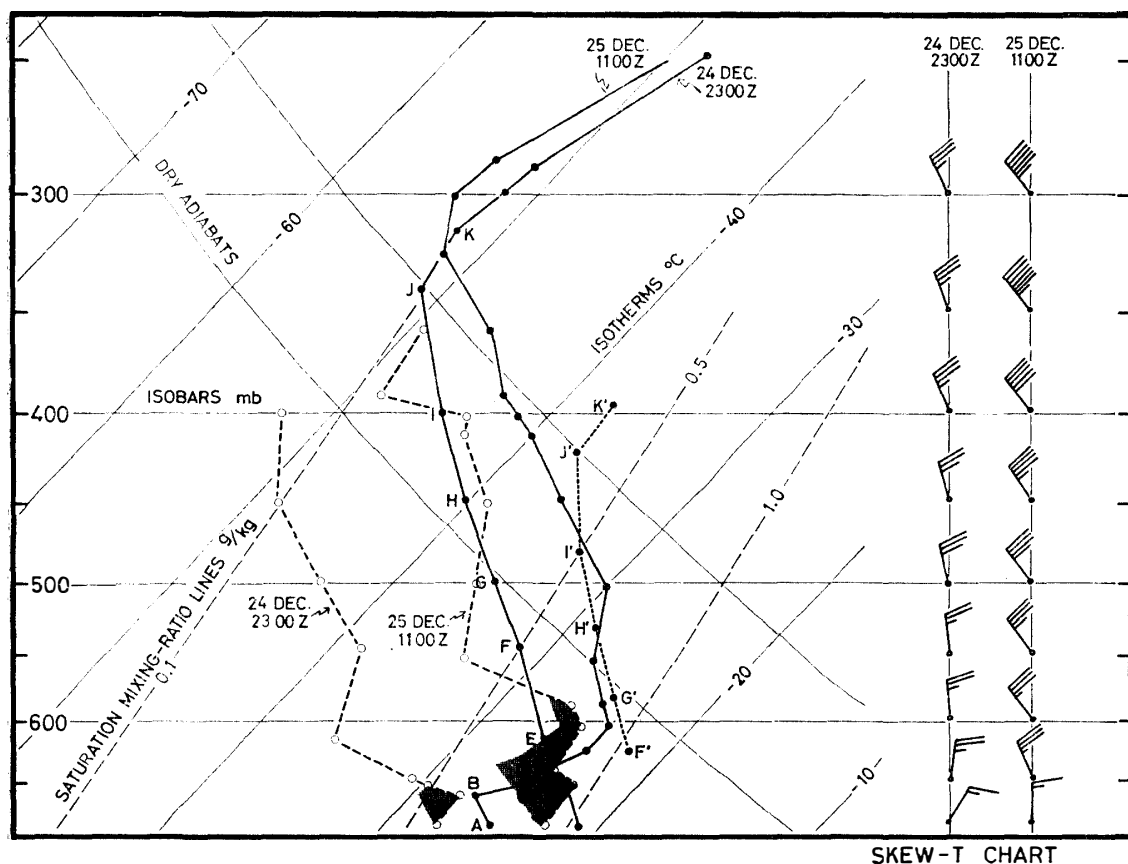


Fig. 7. A Skew-T, Log-P diagram shows temperatures, mixing ratios and winds aloft at 2300 GMT, December 24, and at 1100 GMT, December 25.

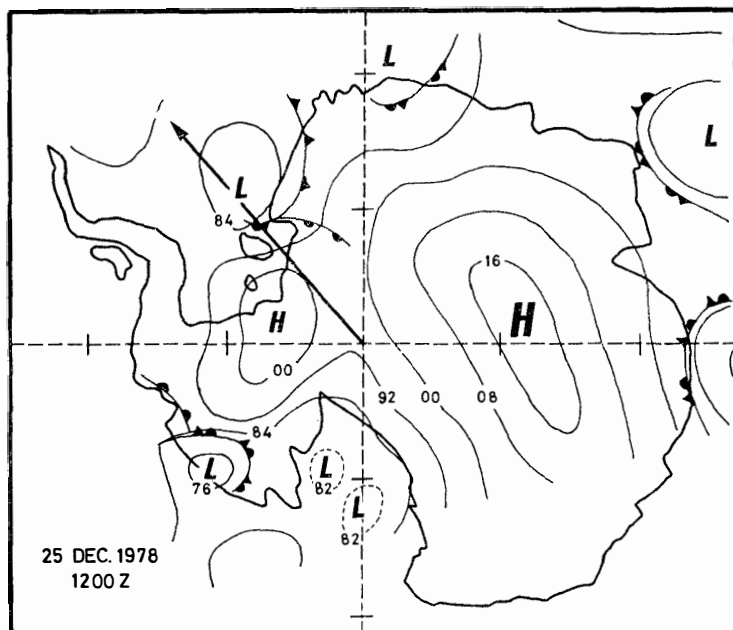


Fig. 8a. Sea-level pressure chart at 1200 GMT, December 25. The thermal wind direction is shown by an arrow.

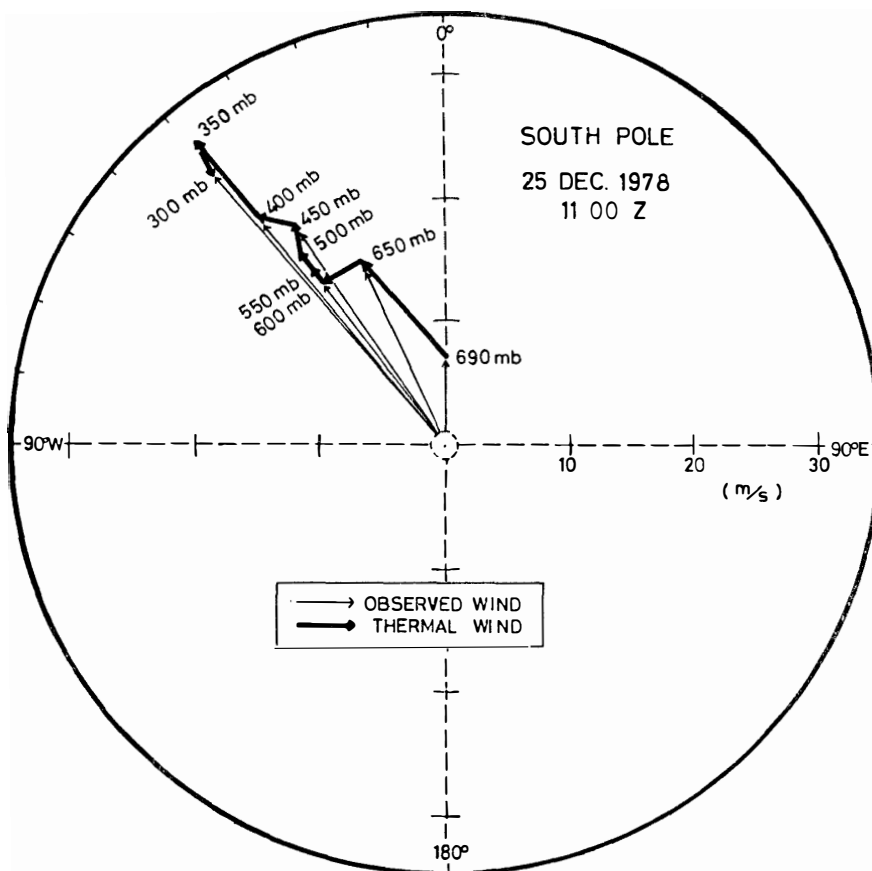


Fig. 8b. Hodograph of geostrophic winds from 600 to 350 mb with precipitation from clouds at 1100 GMT, December 25.

Fig. 8b. As is obvious from Fig. 8a, the thermal wind points the cyclone over the Weddell Sea.

A postulated mechanism of precipitation onto the Antarctic caused by air mass subsidence (*e.g.*, KIKUCHI and HOGAN, 1976; KATO and HIGUCHI, 1979) could partly apply to a change in temperature profiles. If the temperature profile *F* to *K* (solid line) at 2300 GMT, subsided by 80 mb, it changed to the profile *F'* to *K'* (broken line) in Fig. 7; this profile corresponded to the temperature profile 350 mb at 1100 GMT. This layer is attributed to the subsidence of air mass corresponding to the straight thermal layer wind from 600 to 350 mb.

Although the temperature profiles in Fig. 7 bring about precipitation at the South Pole, a further insight can be gained by including humidity data aloft as well. The mixing ratio aloft must be decreased or conserved while a single air mass with or without saturated air subsides. In Fig. 7, however, the mixing ratio increased rapidly, which introduces another mechanism of precipitation.

3.4. Mean humidity and wind fields above the South Pole

For examining the mean humidity field above the South Pole during the austral summer, the time section of the profile of the residue, which is represented by the mixing ratio, was calculated from routine radiosonde observations, as shown in Fig. 9. Water-rich layers supersaturated with respect to ice mainly exist from the surface 2854 m above mean sea level (altitude of South Pole Station) to about 4000 m as is evident from the figure.

The strength of precipitation seems to be closely related to the total amount of precipitable ice in a vertical column of air. The precipitable ice in the profiles of the residue, which is represented by the mixing ratio was integrated, from the snow

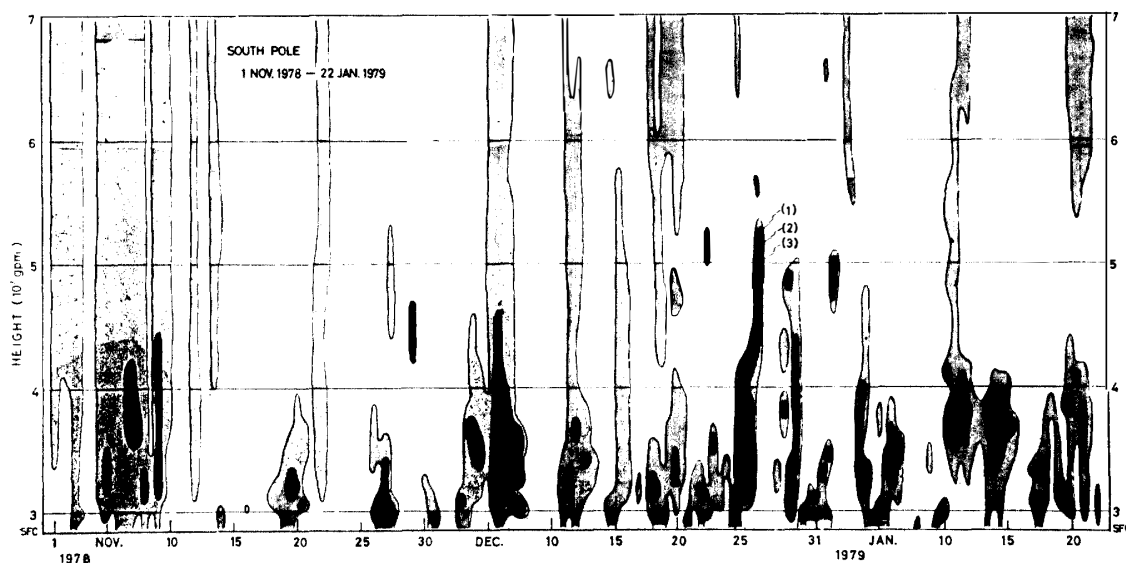


Fig. 9. Time section of mixing ratio profile. The amount of precipitable ice is shaded as follows:
 (1): mixing ratio from ice saturation to 0.1 g/kg;
 (2): mixing ratio from 0.1 to 0.2 g/kg;
 (3): mixing ratio from 0.2 g/kg to water saturation.

surface to the tropopause, and the result shown in Fig. 10. Every twelve hours the amount of precipitable ice varied from zero to 0.3 mm. Broken lines show dates of occurrence of clear sky precipitation as mentioned in Section 3.1. In the bottom column open and a shaded spaces show dates when the cloud amount was not larger than one tenth and not smaller than two-tenths, respectively. The frequency of occurrence of a sky that cleared up, with the cloud amount not larger than one tenth, was about 25 percent during austral summer 1978–1979 at the South Pole. Therefore, the frequency of occurrence of clear sky precipitation is estimated to be about one third the number of occurrences of a clear sky both in cases with and without precipitation. The cloud amount shows a good correlation with the amount of precipitable ice; the presence of precipitable ice in a vertical column of air corresponds to the frequency of occurrence of cloudy weather.

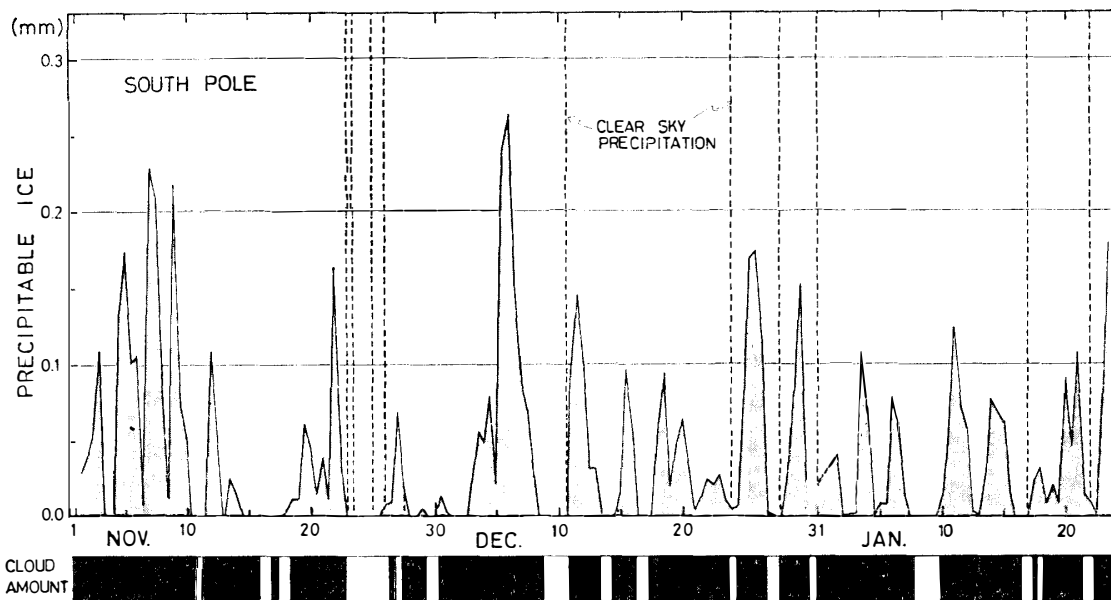


Fig. 10. Time series of precipitable ice and the cloud amount.

“Cloudy days”, whose cloud amount were more than one tenth, appeared at more or less fixed interval. According to a spectral analysis using data at Mizuho Station, which is about 300 km inland from Syowa Station, East Antarctica, a predominant period lasting three to four days in surface meteorological elements such as atmospheric pressure, temperature and wind speed is attributed to synoptic-scale disturbances passing the coastal region near Syowa Station (INOUE *et al.*, 1978). Air masses with precipitable ice seems to be associated with the behavior of eddies.

An inspection of the mean geostrophic wind will provide useful information on an air mass in advective flow. The wind rose at 500 mb, which is representative of geostrophic winds aloft, is shown to have two patterns in Fig. 11. One is based on all data throughout the three months from November 1978 to January 1979; the other is based on selected data only, obtained when weather cleared up during the same months. It is obvious that the latter shifts considerably to the east compared with the former; generally speaking, predominant winds aloft blow from the NW

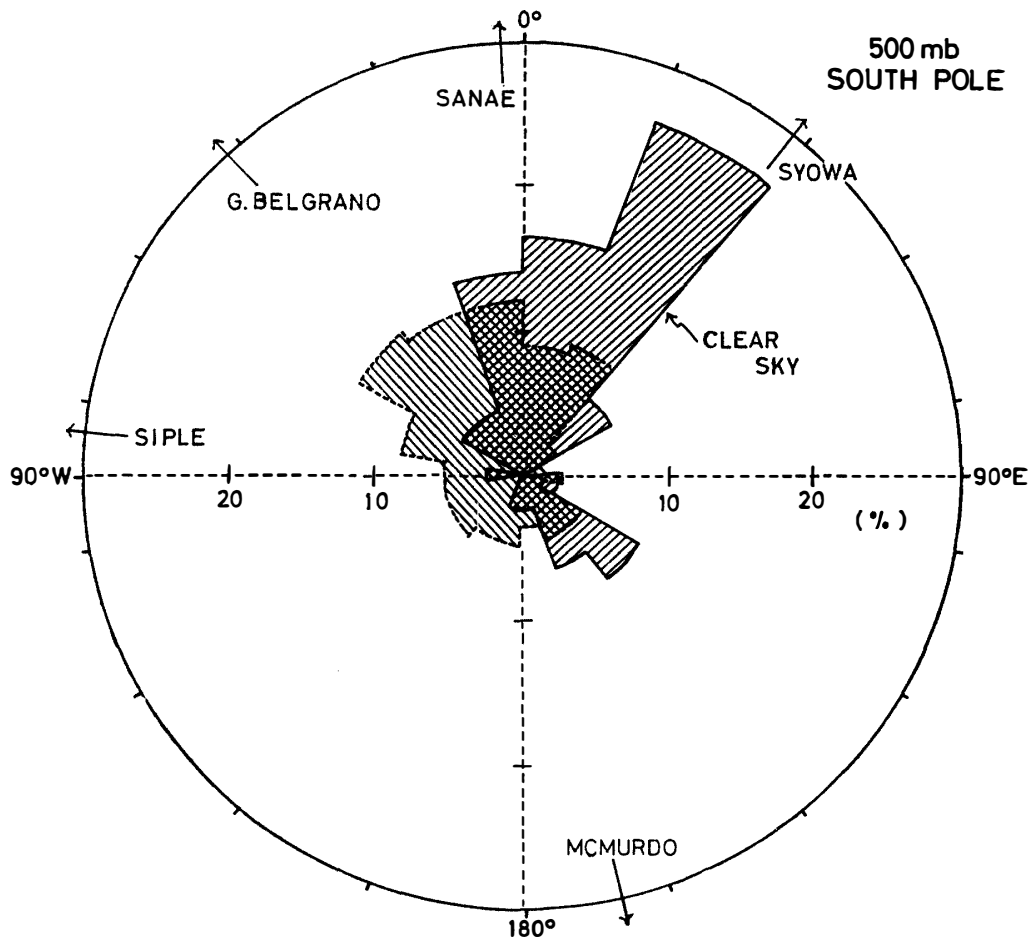


Fig. 11. Two kinds of wind roses at the 500 mb surface: one is based on all data from November 1978 to January 1979; the other is based on the selected data only when the sky cleared up during the same period.

(from the direction of the Weddell Sea). On the other hand, when the sky cleared, winds blow from the NE (from the interior region).

Water mass flux is plotted against wind direction at 500 mb, as shown in Fig. 12. Solid and open circles indicate the existence and the nonexistence of layers supersaturated with respect to ice, respectively. The direction shaded, pointing to the Weddell Sea, abounds in solid circles, which imply the transport of wet air masses associated with precipitation. It is assumed that wet air masses, which move in advective flow from the coast to the South Polar Plateau, rise along the slope and cool there. On the other hand, the NE direction pointing to the interior region abounds in open circles. Upper winds, when the sky has cleared up, are mostly suited to transport of dry air masses to the South Polar Plateau over a longer distance from the Indian Ocean via the interior region than those from the Weddell Sea or the Ross Sea. Therefore, the difference in moisture above the South Pole is due to the difference in the sources of air masses.

Clear sky precipitation is considered a transition phenomenon from when the sky [has cleared up to when it is cloudy, and *v.v.*; in other words, a transition

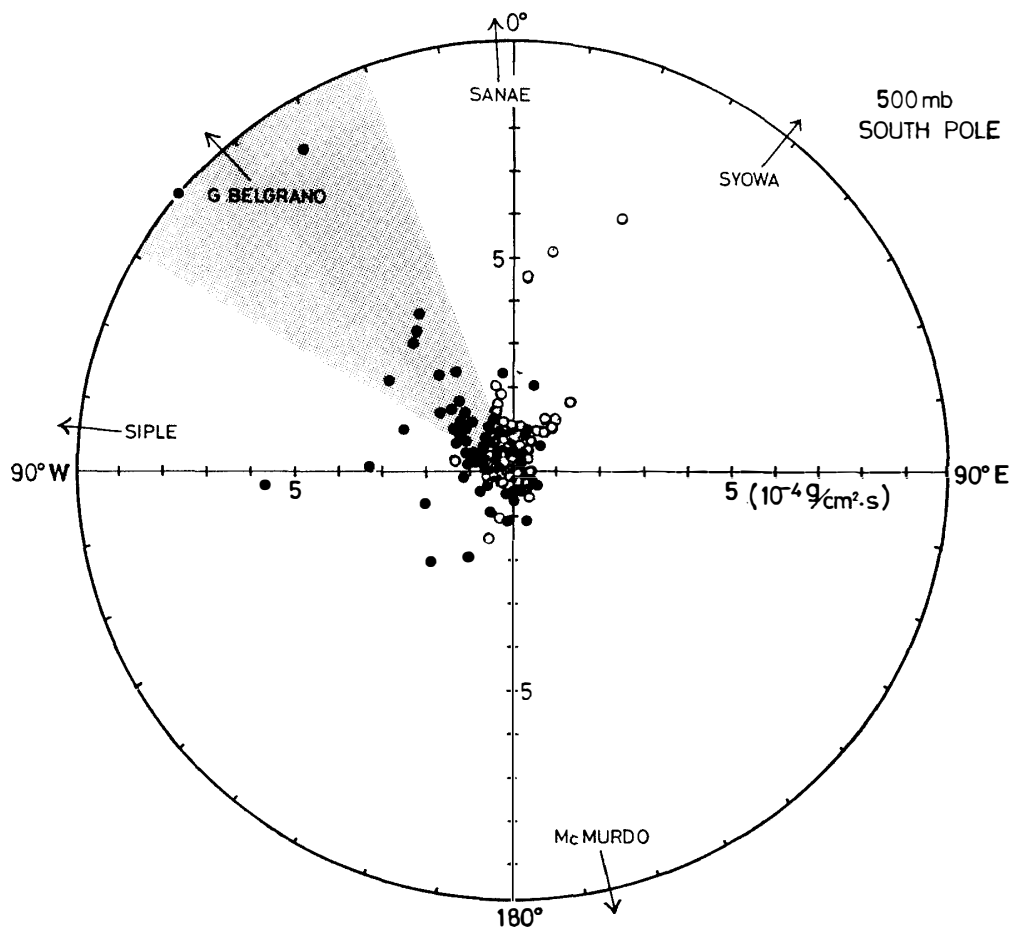


Fig. 12. Water mass flux vs. wind direction at 500 mb: Solid and open circles indicate the existence and the nonexistence of layers supersaturated with respect to ice, respectively.

phenomenon from a dry atmosphere without precipitable ice to an atmosphere with abundant water, and *v.v.* This notion of transition explains why the lifetime of clear sky precipitation was observed to be several hours, it occurred immediately before and after precipitation from clouds, and ice crystals in the forms of thin hexagonal plates and columns were observed both from stratus-type clouds and a clear sky.

4. Concluding Remarks

This study, done in the austral summer, disclosed that the South Pole is occasionally influenced by frontal activities deriving from the Weddell and Ross Seas. The mechanism of precipitation from a cloudy sky onto the South Polar Plateau is related to advection of moist air masses driven by eddies around the coast.

The occurrence of clear sky precipitation onto the South Polar Plateau is not rare. The mechanism of clear sky precipitation has aroused considerable attention on the part of polar meteorologist, because of its scientific curiosity. But the mechanism has not been clear.

The following is our conclusion concerning clear sky precipitation: Whenever it is observed, the surface weather is calm and isotherms veer to easterly from 600 to 300 mb; during the precipitation, halos are noticed, a small amount of stratus is always detected immediately above the horizon around the South Pole, and ice crystals in the forms of thin hexagonal plates and columns are observed. Clear sky precipitation can be caused by a thin layer supersaturated with respect to ice which is always found immediately above the snow surface; this layer is so thin and contains such a small amount of precipitable ice that it is not identifiable as a cloud; other characteristics of precipitation from this layer are, except for its short lifetime of several hours, much the same as those of precipitation from stratus-type clouds.

Clear sky precipitation is considered a transition phenomenon from when the sky cleared up to when it is cloudy, and *v.v.* Clear sky ice crystals at the South Pole may result from freezing of low-level stratus cloud droplets, which form from an air mass transported from the highest interior region along the slight slope toward the South Polar Plateau.

As more data become available, the study of precipitation will be broadened to cover other regions of Antarctica, using the result of this study as a stepping stone.

Acknowledgments

The authors wish to express their thanks to Mr. B. O'HANLON of the USN Meteorological Detachment and Mr. S. VERNARD of New York University for assistance they generously gave at South Pole Station from November 1978 to January 1979. Logistic service was provided to this study by the Division of Polar Programs of the National Science Foundation.

References

- HINDMAN, E. E. and RINKER, R. I. (1967): Continuous snowfall replicator. *J. Appl. Meteorol.*, **6**, 126–133.
- HOGAN, A. W. (1979): Meteorological transport of particulate material to the South Polar Plateau. *J. Appl. Meteorol.*, **18**, 741–749.
- INOUE, M., YAMADA, T. and KOBAYASHI, S. (1978): Effects of synoptic scale disturbance on seasonal variations of katabatic winds and moisture transport into Mizuho Plateau. *Mem. Natl Inst. Polar Res., Spec. Issue*, **7**, 101–114.
- ITOO, K. (1951): Phenomena of ice crystals in the air (On small ice crystals-1). *Pap. Meteorol. Geophys.*, **2**, 67–75.
- KATO, K. and HIGUCHI, K. (1979): Nankyoku kôkiatsu-ka de seisei shita yuki no sanso dôitai sosei (Oxygen isotopic composition of snow formed under an Antarctic anticyclone). *Nankyoku Shiryô (Antarct. Rec.)*, **67**, 152–163.
- KIKUCHI, K. and HOGAN, A. W. (1976): Snow crystal observations in summer season at Amundsen-Scott South Pole Station, Antarctica. *J. Fac. Sci., Hokkaido Univ., Ser. 7*, **5**, 1–20.
- KUHN, M. (1970): Ice crystals and solar halo displays, Plateau Station, 1967. *International Symposium on Antarctic Glaciological Exploration (ISAGE)*, Hanover, New Hampshire, 1968, ed. by A. J. Gow *et al.* Cambridge, Heffer, 298–303 (Publ. No. 86).
- KUTZBACH, G. and SCHWERDTFEGER, W. (1967): Temperature variations and vertical motion in the free atmosphere over Antarctica in the winter. *Proc. Symp. Polar Meteorol.*, Geneva 1966, *World Meteorol. Organ., Tech. Note*, **87**, 225–248.

- LAX, J. N. and SCHWERDTFEGER, W. (1976): Terrain-induced vertical motion and occurrence of ice crystal fall at South Pole in summer. *Antarct. J. U.S.*, **11**, 144–145.
- OHTAKE, T. (1976): Ice crystals in the Antarctic atmosphere. *Proc. Int. Conf. Cloud Physics*, Boulder, Colo., July 1976, 484–487.
- OHTAKE, T. and HOLGREN, B. E. (1974): Ice crystals from a cloudless sky. *Conf. Cloud Physics*, Am. Meteorol. Soc., Tucson, Arizona, Oct. 1974, 317–320.
- OHTAKE, T. and INOUE, M. (1980): Formation mechanism of ice crystal precipitation in the Antarctic atmosphere. *Proc. Int. Conf. Cloud Physics*, Clemert-Ferrand, July 1980, 221–224.
- OHTAKE, T. and JAYAWEERA, K. O. L. F. (1972): Ice crystal displays from power plants. *Weather*, **27**, 271–277.
- RUBIN, M. J. and WEYANT, W. S. (1963): The mass and heat budget of the Antarctic atmosphere. *Mon. Weather Rev.*, **91**, 487–493.
- RUSIN, N. P. (1964): *Meteorological and Radiational Regime of Antarctica*. Jerusalem, IPST, 355 p.
- SCHWERDTFEGER, W. (1969): Ice crystal precipitation on the Antarctic plateau. *Antarct. J. U.S.*, **4**, 221–222.
- WEXLER, H., MORELAND, W. B. and WEYANT, W. S. (1960): A preliminary report on ozone observations at Little America, Antarctica. *Mon. Weather Rev.*, **88**, 43–54.

(Received April 2, 1984; Revised manuscript received August 28, 1984)